



High order finite volume WENO schemes for the shallow water flows through channels with irregular geometry



Yulong Xing

Department of Mathematics, University of California Riverside, Riverside, CA 92521, USA

ARTICLE INFO

Article history:

Received 30 May 2015

Received in revised form 30 November 2015

Keywords:

Shallow water flows

Cross section

Well-balanced

WENO scheme

Finite volume method

Positivity-preserving

ABSTRACT

The shallow water equations are widely used to model flows in rivers and coastal areas. In this paper, we consider the shallow water flows in open channels with irregular geometry and a non-flat bottom topography, and design high order finite volume weighted essentially non-oscillatory (WENO) methods. A special source term approximation is introduced so that the proposed methods can preserve the still water steady state exactly. We also employ a simple positivity-preserving limiter to provide efficient and robust simulations near the wetting and drying front. The proposed methods are well-balanced for the still water steady state solutions, preserve the non-negativity of the wet cross section, and are genuinely high order accurate in smooth regions for general solutions and essentially non-oscillatory for general solutions with discontinuities. Numerical examples are performed at the end to verify these properties.

© 2015 Elsevier B.V. All rights reserved.

1. Introduction

The shallow water equations are widely used in the modeling and simulation of free surface flows in rivers and coastal areas, and can predict tides, storm surge levels and coastline changes from hurricanes and ocean currents. In this paper, we consider shallow water flows in open channels with irregular geometry and a non-flat bottom topography, which take the form

$$H_t + Q_x = 0 \quad (1.1)$$

$$Q_t + \left(\frac{Q^2}{H} + \frac{1}{2}g\sigma h^2 \right)_x = \frac{1}{2}gh^2\sigma_x - g\sigma hb_x$$

where h denotes the water height, b represents the bottom topography, σ is the breadth of the rectangular channel, $H = \sigma h$ is the wet cross section, $Q = Hu$ is the mass flow rate, u is the velocity, and g is the gravitational constant. The source term $-g\sigma hb_x$ accounts for the effect of non-flat bottom topography, and the other source term $gh^2\sigma_x/2$ comes from the variation of the cross section. Other source terms, such as a friction term, could also be added. When the cross section $\sigma(x)$ is a constant, this model reduces to the shallow water equations with a non-flat bottom topography.

For the shallow water equations and other conservation laws with source terms, one main difficulty in solving them numerically is the treatment of source terms, which need to be balanced by the flux gradients at the steady state. Otherwise, these methods may introduce spurious oscillations near the steady state, making it challenging to simulate small perturbations of such state. Well-balanced schemes are specially designed to preserve exactly these steady state solutions up to machine error with relatively coarse meshes, and have been an active research area in the past two decades. Many

E-mail address: xingy@ucr.edu.

researchers have developed well-balanced methods for the shallow water equations using different approaches. We refer the readers to [1–6] and the references therein. Another challenge encountered in the simulations of the shallow water model is the appearance of dry or near-dry areas, where no or little water is present. Numerically, negative water height may be produced if no special attention is paid in such area, which may cause the computation to fail as the system loses its hyperbolicity. Various positivity-preserving techniques have been studied to overcome this difficulty, and we refer to [7–11] for some recent related work.

Most of the above work is for the shallow water equations. For the shallow water flow in open channels (1.1), less work can be found in the literature. Vázquez–Cendón [12] presented a well-balanced method by rewriting the model in an equivalent form with computational variables (h , hu) and two additional source terms which account for the variable cross section $\sigma(x)$ and are zero at the steady state. Any well-balanced method for the shallow water equations can be extended here directly. Well-balanced methods based on extensions of Roe's discretization with proper flux difference splitting were given in [13]. Balbás and Karni [14] presented second-order well-balanced positivity-preserving numerical methods for the shallow water flow in rectangular channels, extending the results for the shallow water equations in [9]. Later, Hernández-Duenas and Karni [15] extended their results to the shallow water flow with arbitrary cross section, and designed well-balanced Roe-type upwind methods. Murillo and García-Navarro [16] recently proposed well-balanced method based on energy balanced arguments.

High-order accurate numerical schemes (with higher than second-order accuracy) have attracted increasing attention in many computational fields. Examples include finite difference/volume weighted essentially non-oscillatory (WENO) schemes, spectral methods and discontinuous Galerkin (DG) methods. They have been applied to solve the shallow water equations, and some of them are well-balanced and positivity-preserving, but we do not see such methods for the shallow water flow in channels. The main objective of this paper is to develop high-order finite volume WENO methods for the shallow water flows (1.1) in open channels with rectangular cross section. The proposed methods are genuinely high-order, well-balanced for the steady state solution and preserve the non-negativity of the wet cross section without loss of mass conservation.

This paper consists of four additional sections. In Section 2, the mathematical model and its steady state solutions are described. The well-balanced algorithm is presented in Section 3. We propose a novel source term approximation, which is not only high order accurate, but also well-balanced. Coupled with well-balanced numerical fluxes, the resulting WENO methods are shown to capture the steady state solution exactly. In Section 4, we demonstrate that the first order version of the proposed methods preserves the non-negativity of water height, and then show that, high order WENO methods, coupled with a simple positivity-preserving limiter, maintain this property. The positivity-preserving limiter keeps the water height non-negative, preserves the mass conservation and at the same time does not affect the high-order accuracy for the general solutions. Finally, in Section 5 we provide some numerical experiments to gauge the performance of the proposed well-balanced positivity-preserving WENO methods for the shallow water model in open channels, demonstrating the accuracy and robustness of the proposed methods for a wide range of shallow water flows.

2. The shallow water model in open channels

As simplified models of some free surface flows, the shallow water equations for flows in an open channel with variable cross section take the form

$$\begin{aligned} H_t + Q_x &= 0 \\ Q_t + \left(\frac{Q^2}{H} + I_1 \right)_x &= I_2 - g\sigma_b h b_x, \end{aligned} \quad (2.1)$$

where $\sigma^0(x, z)$ is the breadth of the channel, $\sigma_b(x) = \sigma^0(x, b(x))$ is the bottom channel width, $H = \int_b^{h+b} \sigma^0(x, z) dz$ is the cross-sectional wet area, and $Q = Hu$ is the mass flow rate. I_1 is given by $I_1 = g \int_h^{h+b} (h + b - z) \sigma^0(x, z) dz$ which is equal to the cross-sectional average of the hydrostatic pressure multiplied by H , and $I_2 = g \int_h^{h+b} (h + b - z) \sigma_x^0(x, z) dz$.

The Eqs. (2.1) have the hydrostatic pressure that cannot be directly expressed in terms of the computational variables (H , Q). By some simple algebra, one can show that it is equivalent to the following non-conservative formation:

$$\begin{aligned} H_t + Q_x &= 0 \\ Q_t + \left(\frac{Q^2}{H} \right)_x + \frac{g}{2\sigma_t} (H^2)_x &= \frac{gH}{\sigma_t} (I_3 - \sigma_b b_x), \end{aligned} \quad (2.2)$$

which can be further written in the matrix form:

$$\begin{pmatrix} H \\ Q \end{pmatrix}_t + \begin{pmatrix} 0 & 1 \\ u^2 - c_0^2 & 2u \end{pmatrix} \begin{pmatrix} H \\ Q \end{pmatrix}_x = \begin{pmatrix} 0 \\ c^2 (I_3 - \sigma_b b_x) \end{pmatrix}, \quad (2.3)$$

where $\sigma_t(x) = \sigma^0(x, h(x) + b(x))$, $c_0^2 = gH/\sigma_t$, and $I_3 = \int_b^{h+b} \sigma_x(x, z) dz$. Numerical methods for the non-conservative hyperbolic system remain a difficult task, although there have been some recent developments along this direction [17, 18].

In this paper, we consider the flows in channel with rectangular cross section, i.e. $\sigma^0(x, z) \equiv \sigma(x)$, where the hydrostatic pressure can be written as a function of variables and the model becomes a system of standard conservation laws. Under this case, we have $\sigma_b(x) = \sigma(x)$, $H = \sigma h$, $I_1 = g\sigma h^2/2$, $I_2 = g\sigma_x h^2/2$, and the model (2.1) can be reduced to (1.1), which is equivalent to

$$\begin{pmatrix} H \\ Q \end{pmatrix}_t + \begin{pmatrix} 0 & 1 \\ u^2 - c^2 & 2u \end{pmatrix} \begin{pmatrix} H \\ Q \end{pmatrix}_x = \begin{pmatrix} 0 \\ gh^2\sigma_x - gh\sigma b_x \end{pmatrix}, \tag{2.4}$$

with $c^2 = gh$. The system is hyperbolic, and has two eigenvalues given by $u \pm \sqrt{gh}$. Note that when the channel width σ is a constant and independent of x , the model (2.1) or (1.1) becomes the well-known shallow water equations with a non-flat bottom topography.

Like the shallow water equations, the shallow water model (1.1) in rectangular channel admits the general moving water steady state solutions which take the form of

$$Q = \text{const}, \quad \frac{1}{2}u^2 + g(h + b) = \text{const}. \tag{2.5}$$

Special attention is often given to the still water steady state solution,

$$u = 0, \quad h + b = \text{const}, \tag{2.6}$$

which is a special case when the velocity reduces to zero, and represents a still flat water surface. Well-balanced methods for the still water steady state solution (2.6) will be discussed in the next section.

3. Well-balanced finite volume WENO methods

Finite volume schemes are very popular for solving hyperbolic conservation laws. In this section, we present high order well-balanced finite volume WENO schemes for the shallow water flows (1.1) in open channels. Well-balanced numerical flux following the hydrostatic reconstruction technique, and a high order novel well-balanced source term approximation constitute the key components in designing our well-balanced methods.

3.1. Notations and review of WENO methods

We discretize the computational domain into cells $I_j = [x_{j-\frac{1}{2}}, x_{j+\frac{1}{2}}]$, and denote the size of the j th cell by Δx_j and the maximum mesh size by $\Delta x = \max_j \Delta x_j$. For the ease of presentation, we denote the shallow water model (1.1) by

$$U_t + f(U, \sigma)_x = s(U, \sigma, b)$$

where $U = (H, Q)^T = (\sigma h, \sigma hu)^T$ with the superscript T denoting the transpose, $f(U, \sigma) = (Q, Hu^2 + g\sigma h^2/2)^T$ is the flux and $s(U, \sigma, b) = (0, gh^2\sigma_x/2 - g\sigma hb_x)^T$ is the source term. Our computational variables in finite volume schemes are $\bar{U}_j(t)$, which approximate the cell averages of the exact solution, $\bar{U}(x_j, t) = \frac{1}{\Delta x_j} \int_{I_j} U(x, t) dx$. The conservative finite volume numerical scheme then takes the form

$$\frac{d}{dt} \bar{U}_j(t) + \frac{1}{\Delta x_j} (\hat{f}_{j+\frac{1}{2}} - \hat{f}_{j-\frac{1}{2}}) = \frac{1}{\Delta x_j} \int_{I_j} s(U, \sigma, b) dx, \tag{3.1}$$

with $\hat{f}_{j+\frac{1}{2}} = F(U_{j+\frac{1}{2}}^-, U_{j+\frac{1}{2}}^+; \sigma_{j+\frac{1}{2}}^-, \sigma_{j+\frac{1}{2}}^+)$ being the numerical flux. One of the simplest and most inexpensive numerical fluxes is the Lax–Friedrichs flux. $U_{j+\frac{1}{2}}^-$ and $U_{j+\frac{1}{2}}^+$ are the high-order pointwise approximations to $U(x_{j+\frac{1}{2}}, t)$ from left and right respectively, and are computed through the neighboring cell average values $\bar{U}_{j\pm r}$ by a high-order WENO reconstruction procedure. If we want to obtain $(2k - 1)$ th order WENO schemes, we would first compute reconstructed boundary values $U_{j+\frac{1}{2}}^{(k),\pm}$ using different candidate stencils. Then by providing each boundary value a positive weight which indicates the smoothness of its corresponding stencil, we define the WENO reconstructed $U_{j+\frac{1}{2}}^\pm$ as a convex combination of all these k reconstructed values. Eventually, we can write the WENO reconstruction procedure as:

$$U_{j+\frac{1}{2}}^+ = \sum_{r=-k+1}^k w_r \bar{U}_{j+r}, \quad U_{j+\frac{1}{2}}^- = \sum_{r=-k}^{k-1} \tilde{w}_r \bar{U}_{j+r} \tag{3.2}$$

where $k = 3$ for the fifth order WENO approximation. The coefficients w_r and \tilde{w}_r depend nonlinearly on the smoothness indicators involving the cell average \bar{U} , and satisfy $\sum_{r=-k+1}^k w_r = \sum_{r=-k}^{k-1} \tilde{w}_r = 1$. For hyperbolic system, the local characteristic decomposition, which is more robust than a component by component version, is usually used in the computation. We refer the complete WENO algorithm to the classical papers [19,20].

Total variation diminishing (TVD) high-order Runge–Kutta time discretization [21] is often coupled with the WENO scheme in practice, for stability and to increase temporal accuracy. In this paper, we consider the third order TVD Runge–Kutta method in the numerical tests:

$$\begin{aligned} U^{(1)} &= U^n + \Delta t \mathcal{F}(U^n) \\ U^{(2)} &= \frac{3}{4}U^n + \frac{1}{4}(U^{(1)} + \Delta t \mathcal{F}(U^{(1)})) \\ U^{n+1} &= \frac{1}{3}U^n + \frac{2}{3}(U^{(2)} + \Delta t \mathcal{F}(U^{(2)})), \end{aligned} \tag{3.3}$$

where $\mathcal{F}(U)$ is the spatial operator.

3.2. Reconstruction and well-balanced fluxes

In order to achieve the well-balanced property, we are interested in preserving the still water stationary solution (2.6) exactly. Well-balanced finite volume WENO methods have been designed in [22,23] for the shallow water equations with a non-flat bottom, and our methods are built based on them. Similar to all other methods following the hydrostatic reconstruction techniques [2], our well-balanced methods have the form

$$\frac{d}{dt} \bar{U}_j + \frac{1}{\Delta x_j} (\hat{f}_{j+\frac{1}{2}}^l - \hat{f}_{j-\frac{1}{2}}^r) = \frac{1}{\Delta x_j} \int_{I_j} s(U, \sigma, b) dx. \tag{3.4}$$

First, we want to recover the steady state solution at each time level using the computational variables \bar{U}_j . The steady state (2.6) is given by $H/\sigma + b = h + b = \text{const}$, and we denote that constant by C . It is well-known that the cell averages of these functions do not satisfy the same equality, i.e., $\bar{H}_j/\bar{\sigma}_j + \bar{b}_j \neq C$. Therefore, we introduce the new variable

$$B(x) = \sigma(x)b(x),$$

which does not change in time, and we have $(\bar{H}_j + \bar{B}_j)/\bar{\sigma}_j = C$ at the steady state solution.

Next, we apply the WENO reconstruction to obtain $U_{j+\frac{1}{2}}^\pm$. We hope the reconstructed cell boundary values satisfy an analogue of the steady state solution (2.6), which will be utilized in designing the well-balanced fluxes and source term approximation. Following the idea in [23], we propose to apply the WENO reconstruction on the variables $V = (H + B, Q)^T$ to obtain $(H + B)_{j+\frac{1}{2}}^\pm$ and $Q_{j+\frac{1}{2}}^\pm$, i.e.,

$$V_{j+\frac{1}{2}}^+ = \sum_{r=-k+1}^k w_r \bar{V}_{j+r}, \quad V_{j+\frac{1}{2}}^- = \sum_{r=-k}^{k-1} \tilde{w}_r \bar{V}_{j+r}. \tag{3.5}$$

We also apply the same coefficients w_r and \tilde{w}_r used in (3.5) on $\Gamma = (\sigma, 0)^T$ to obtain $\sigma_{j+\frac{1}{2}}^\pm$ by

$$\Gamma_{j+\frac{1}{2}}^+ = \sum_{r=-k+1}^k w_r \bar{\Gamma}_{j+r}, \quad \Gamma_{j+\frac{1}{2}}^- = \sum_{r=-k}^{k-1} \tilde{w}_r \bar{\Gamma}_{j+r}. \tag{3.6}$$

Note that these coefficients w_r and \tilde{w}_r depend nonlinearly on the variables \bar{V}_j . Hence, at the steady state when the solutions satisfy $\bar{Q}_j = 0, \bar{H}_j + \bar{B}_j = C \bar{\sigma}_j$, we have

$$\frac{V_{j+\frac{1}{2}}^+}{\Gamma_{j+\frac{1}{2}}^+} = \frac{\sum_{r=-k+1}^k w_r \bar{V}_{j+r}}{\sum_{r=-k+1}^k w_r \bar{\Gamma}_{j+r}} = C, \quad \frac{V_{j+\frac{1}{2}}^-}{\Gamma_{j+\frac{1}{2}}^-} = \frac{\sum_{r=-k}^{k-1} \tilde{w}_r \bar{V}_{j+r}}{\sum_{r=-k}^{k-1} \tilde{w}_r \bar{\Gamma}_{j+r}} = C,$$

which give us the same constant C . At the initial time $t = t_0$, we either construct or use the exact bottom topography $b(x)$ to obtain the values $b_{j+\frac{1}{2}}^\pm$ at the cell boundary. Let us now define

$$h_{j+\frac{1}{2}}^\pm = \frac{(H + B)_{j+\frac{1}{2}}^\pm}{\sigma_{j+\frac{1}{2}}^\pm} - b_{j+\frac{1}{2}}^\pm, \quad B_{j+\frac{1}{2}}^\pm = \sigma_{j+\frac{1}{2}}^\pm b_{j+\frac{1}{2}}^\pm,$$

and from above we know that the reconstructed values satisfy $h_{j+\frac{1}{2}}^\pm + b_{j+\frac{1}{2}}^\pm = C, u_{j+\frac{1}{2}}^\pm = 0$ at the still water steady state (2.6). Note that in this procedure, although $(\bar{H}_j + \bar{B}_j)/\bar{\sigma}_j = C$ at the steady state, we cannot apply the reconstruction on them directly to obtain the reconstructed cell boundary values, since they are only second order approximations to the cell average of $(H + B)/\sigma$.

Now we are ready to present the well-balanced fluxes, following the idea of hydrostatic reconstruction idea used in [2,6]. We first define $\sigma^* = \min(\sigma_{j+\frac{1}{2}}^+, \sigma_{j+\frac{1}{2}}^-)$, set

$$H_{j+\frac{1}{2}}^{*,\pm} = \max\left(0, \sigma_{j+\frac{1}{2}}^*(h+b)_{j+\frac{1}{2}}^\pm - \max(B_{j+\frac{1}{2}}^+, B_{j+\frac{1}{2}}^-)\right) \tag{3.7}$$

and redefine the left and right values of U as:

$$U_{j+\frac{1}{2}}^{*,\pm} = \begin{pmatrix} H_{j+\frac{1}{2}}^{*,\pm} \\ H_{j+\frac{1}{2}}^{*,\pm} u_{j+\frac{1}{2}}^\pm \end{pmatrix}. \tag{3.8}$$

Then the left and right fluxes $\widehat{f}_{j+\frac{1}{2}}^l$ and $\widehat{f}_{j-\frac{1}{2}}^r$ are given by:

$$\widehat{f}_{j+\frac{1}{2}}^l = F(U_{j+\frac{1}{2}}^{*, -}, U_{j+\frac{1}{2}}^{*, +}; \sigma_{j+\frac{1}{2}}^*, \sigma_{j+\frac{1}{2}}^*) + \begin{pmatrix} 0 \\ \frac{g}{2\sigma_{j+\frac{1}{2}}^-} (H_{j+\frac{1}{2}}^-)^2 - \frac{g}{2\sigma_{j+\frac{1}{2}}^*} (H_{j+\frac{1}{2}}^{*, -})^2 \end{pmatrix} \tag{3.9}$$

$$\widehat{f}_{j-\frac{1}{2}}^r = F(U_{j-\frac{1}{2}}^{*, -}, U_{j-\frac{1}{2}}^{*, +}; \sigma_{j-\frac{1}{2}}^*, \sigma_{j-\frac{1}{2}}^*) + \begin{pmatrix} 0 \\ \frac{g}{2\sigma_{j-\frac{1}{2}}^+} (H_{j-\frac{1}{2}}^+)^2 - \frac{g}{2\sigma_{j-\frac{1}{2}}^*} (H_{j-\frac{1}{2}}^{*, +})^2 \end{pmatrix}. \tag{3.10}$$

The goal of this hydrostatic reconstruction is to let $U^{*, -} = U^{*, +}$ at the steady state, which leads to

$$\widehat{f}_{j+\frac{1}{2}}^l = f(U_{j+\frac{1}{2}}^-, \sigma_{j+\frac{1}{2}}^-), \quad \widehat{f}_{j-\frac{1}{2}}^r = f(U_{j-\frac{1}{2}}^+, \sigma_{j-\frac{1}{2}}^+).$$

Remark 3.1. If the bottom b is continuous, i.e. $b_{j+\frac{1}{2}}^- = b_{j+\frac{1}{2}}^+$, one does not need to introduce this hydrostatic reconstruction, as in [14].

Remark 3.2. As explained in [23,11], $\widehat{f}_{j+\frac{1}{2}}^l - \widehat{f}_{j+\frac{1}{2}}^l$ and $\widehat{f}_{j-\frac{1}{2}}^r - \widehat{f}_{j-\frac{1}{2}}^r$ are both high order correction terms at the level of $O(\Delta x^{2k-1})$ regardless of the smoothness of the solution U . Therefore, the WENO method (3.4) can be rewritten in the form whose left side is the traditional WENO method and right side contains high order approximations to the source term.

3.3. Source term approximation

Next, we present the well-balanced high order approximation of the source term integration. At the steady state (2.6), the balance between the flux and source term reduces to $(\frac{1}{2}g\sigma h^2)_x = \frac{1}{2}g\sigma_x h^2 - g\sigma h b_x$. Let us introduce the notations of

$$Da = a_{j+\frac{1}{2}}^- - a_{j-\frac{1}{2}}^+, \quad \{a\} = \frac{1}{2}(a_{j-\frac{1}{2}}^+ + a_{j+\frac{1}{2}}^-).$$

Using the relation $D(ab) = Da\{b\} + \{a\}Db$, we have

$$D\left(\frac{1}{2}g\sigma h^2\right) = \frac{1}{2}gD\sigma\{h^2\} - \frac{1}{2}g\{\sigma\}D(h^2) = \frac{1}{2}gD\sigma\{h^2\} - g\{\sigma\}\{h\}Dh.$$

Therefore, we can obtain the following second order approximation

$$\begin{aligned} \int_{I_j} \frac{1}{2}g\sigma_x h^2 - g\sigma h b_x dx &\approx S\left(h_{j+\frac{1}{2}}^-, h_{j-\frac{1}{2}}^+\right) \\ &:= \frac{1}{2}g\left(\sigma_{j+\frac{1}{2}}^- - \sigma_{j-\frac{1}{2}}^+\right) \frac{(h_{j+\frac{1}{2}}^-)^2 + (h_{j-\frac{1}{2}}^+)^2}{2} - g \frac{\sigma_{j+\frac{1}{2}}^- + \sigma_{j-\frac{1}{2}}^+}{2} \frac{h_{j+\frac{1}{2}}^- + h_{j-\frac{1}{2}}^+}{2} \left(b_{j+\frac{1}{2}}^- - b_{j-\frac{1}{2}}^+\right), \end{aligned} \tag{3.11}$$

which is the extension of the source term approximation for the shallow water equations presented in [9], and has also been introduced in [14] to design a second order central well-balanced scheme. Easy to verify that at the steady state, we have the desired well-balanced property

$$S\left(h_{j+\frac{1}{2}}^-, h_{j-\frac{1}{2}}^+\right) = f_2\left(U_{j+\frac{1}{2}}^-, \sigma_{j+\frac{1}{2}}^-\right) - f_2\left(U_{j-\frac{1}{2}}^+, \sigma_{j-\frac{1}{2}}^+\right)$$

where f_2 denotes the second flux function.

However, this source term approximation is only second-order accurate. To obtain high order approximation, we can adopt the extrapolation technique used in the paper [24,25]. Let us first subdivide each cell I_j into N subcells and define the following quadrature S_N :

$$S_N = \sum_{l=1}^N S(h_{l-1}, h_l) \tag{3.12}$$

where the subscript l means the value at the point $x_{j-\frac{1}{2}} + l\Delta x/N$. In the case of steady state, S_N is also a second order well-balanced approximation due to the fact that

$$S_N = \sum_{k=1}^N S(h_{k-1}, h_k) = \sum_{k=1}^N (f_2(U_k) - f_2(U_{k-1})) = f_2(U_N) - f_2(U_0) = f_2\left(U_{j+\frac{1}{2}}^-, \sigma_{j+\frac{1}{2}}^-\right) - f_2\left(U_{j-\frac{1}{2}}^+, \sigma_{j-\frac{1}{2}}^+\right).$$

The key idea presented in [24] to derive a high order source term approximation is to employ extrapolation by the linear combination of S_l . For example, a well-balanced fourth order approximation is given by

$$\frac{4S_2 - S_1}{3}. \tag{3.13}$$

Compared with the second order source term discretization S_1 , the fourth order well-balanced scheme needs one additional reconstructed point value at the cell center x_j per cell, which is necessary for the computation of S_2 .

3.4. Summary of the well-balanced scheme

We now summarize the complete procedure of our high order well-balanced WENO methods for solving the shallow water flows (1.1) in open channels with still water steady state solutions. The semi-discrete methods are given by

$$\frac{d}{dt} \bar{U}_j + \frac{1}{\Delta x_j} (\hat{f}_l^l - \hat{f}_r^r) = \frac{1}{\Delta x_j} s_j, \tag{3.14}$$

where the numerical fluxes \hat{f}^l and \hat{f}^r are computed in (3.9)–(3.10), and the source term s_j is defined by the fourth order well-balanced approximation (3.11)–(3.13). The scheme is completed by a temporal TVD Runge–Kutta discretization (3.3).

Collecting the results of the previous subsections, it is straightforward to prove the following:

Proposition 3.1. *The WENO schemes as described above are well-balanced for the still water steady state (2.6).*

Remark 3.3. When the channel width $\sigma(x)$ and the bottom $b(x)$ are both constant, the proposed methods reduce to the traditional WENO schemes. When only $\sigma(x)$ is constant, this becomes the well-balanced WENO methods proposed in [24].

4. Positivity-preserving high-order WENO methods

A simple positivity-preserving limiter, extended from the maximum-principle-preserving limiter in [26], has been proposed and implemented for the shallow water equations in [11,27] for the DG method and in [28] for the WENO scheme. We have shown that this limiter is able to keep the water height non-negative under suitable CFL condition without affecting the mass conservation, and at the same time does not affect the high order accuracy for the general solutions. In this section, we will explore the coupling of this limiter with well-balanced WENO methods presented in Section 3 for the shallow water flows in open channels. As explained in [26,28], we only consider the simple Euler forward in time in this section. The same results can be generalized to TVD high order Runge–Kutta [21] and multi-step [29] time discretizations since these are convex combinations of the Euler forward operators.

We first present the scheme satisfied by the cell averages of the wetted water cross section in well-balanced WENO methods (3.14), by plugging the fluxes (3.9) and (3.10):

$$\bar{H}_j^{n+1} = \bar{H}_j^n - \lambda \left[\hat{F}\left(H_{j+\frac{1}{2}}^{*, -}, u_{j+\frac{1}{2}}^-, H_{j+\frac{1}{2}}^{*, +}, u_{j+\frac{1}{2}}^+\right) - \hat{F}\left(H_{j-\frac{1}{2}}^{*, -}, u_{j-\frac{1}{2}}^-, H_{j-\frac{1}{2}}^{*, +}, u_{j-\frac{1}{2}}^+\right) \right], \tag{4.1}$$

where $\lambda = \Delta x/\Delta t$, $H_{j+\frac{1}{2}}^{*, \pm}$ are defined in (3.7) and

$$\hat{F}\left(H_{j+\frac{1}{2}}^{*, -}, u_{j+\frac{1}{2}}^-, H_{j+\frac{1}{2}}^{*, +}, u_{j+\frac{1}{2}}^+\right) = \frac{1}{2} \left(H_{j+\frac{1}{2}}^{*, -} u_{j+\frac{1}{2}}^- + H_{j+\frac{1}{2}}^{*, +} u_{j+\frac{1}{2}}^+ - \alpha (H_{j+\frac{1}{2}}^{*, +} - H_{j+\frac{1}{2}}^{*, -}) \right) \tag{4.2}$$

with $H_{j+\frac{1}{2}}^{*, \pm}$ defined in (3.7), and $\lambda = \Delta t/\Delta x$. As shown in [11,28,26], one main building block of positivity-preserving methods is to show their first order version maintains the positivity. We have the following lemma, and refer to [11] for the detailed proof in the shallow water equations.

Lemma 4.1. Under the CFL condition $\lambda\alpha \leq 1$, with $\alpha = \max(|u| + \sqrt{gh})$, consider the following scheme

$$H_j^{n+1} = H_j^n - \lambda [\widehat{F}(H_j^{*,+}, u_j^n; H_{j+1}^{*, -}, u_{j+1}^n) - \widehat{F}(H_{j-1}^{*,+}, u_{j-1}^n; H_j^{*, -}, u_j^n)] \tag{4.3}$$

with \widehat{F} the same as in (4.2) and

$$\begin{aligned} H_j^{*,+} &= \max(0, H_j^n + b_j - \max(b_j, b_{j+1})) \\ H_j^{*, -} &= \max(0, H_j^n + b_j - \max(b_{j-1}, b_j)). \end{aligned}$$

If $H_j^n, H_{j\pm 1}^n$ are non-negative, then H_j^{n+1} is also non-negative.

We now consider high order positivity-preserving schemes. From now on, everything follows exactly the same as the approach in [28], and we only present the main idea here. For the $(2k - 1)$ th order WENO methods, we introduce the N -point (with $2N - 3 \geq 2k - 2$) Legendre Gauss–Lobatto quadrature rule on the interval $I_j = [x_{j-\frac{1}{2}}, x_{j+\frac{1}{2}}]$, and denote these quadrature weights as \widehat{w}_r for the interval $[-1/2, 1/2]$ satisfying $\sum_{r=1}^N \widehat{w}_r = 1$. We then introduce the variable

$$\xi_j = \frac{\overline{H}_j^n - \widehat{w}_1 H_{j-\frac{1}{2}}^+ - \widehat{w}_N H_{j+\frac{1}{2}}^-}{1 - \widehat{w}_1 - \widehat{w}_N}, \tag{4.4}$$

and have

$$\overline{H}_j^n = (1 - \widehat{w}_1 - \widehat{w}_N)\xi_j + \widehat{w}_1 H_{j-\frac{1}{2}}^+ + \widehat{w}_N H_{j+\frac{1}{2}}^-. \tag{4.5}$$

Following the approaches in [28], we then have the results:

Proposition 4.1. Consider the scheme (4.1) satisfied by the cell averages of the wetted cross section. Let ξ_j be defined in (4.4). If $H_{j-\frac{1}{2}}^\pm, H_{j+\frac{1}{2}}^\pm$ and ξ_j are all non-negative, then \overline{H}_j^{n+1} is also non-negative under the CFL condition

$$\lambda\alpha \leq \widehat{w}_1. \tag{4.6}$$

To enforce the conditions of this proposition, we need to modify $\overline{H}_{j+\frac{1}{2}}^\pm$ by employing the following positivity-preserving limiter [26,28]:

$$\widetilde{H}_{j-\frac{1}{2}}^+ = \theta \left(H_{j-\frac{1}{2}}^+ - \overline{H}_j^n \right) + \overline{H}_j^n, \quad \widetilde{H}_{j+\frac{1}{2}}^- = \theta \left(H_{j+\frac{1}{2}}^- - \overline{H}_j^n \right) + \overline{H}_j^n, \tag{4.7}$$

where

$$\theta = \min \left\{ 1, \frac{\overline{H}_j^n}{\overline{H}_j^n - m_j} \right\}, \quad m_j = \min(H_{j-\frac{1}{2}}^+, H_{j+\frac{1}{2}}^-, \xi_j). \tag{4.8}$$

We would like to comment that m_j is usually evaluated at all the Gauss–Lobatto points, which may also involve computations of an additional reconstruction polynomial. Here, we only need to evaluate the minimum of three points, making the computation easier. We have shown in [28] that the limiter (4.7) and (4.8) is a high order accurate positivity-preserving limiter. We now have the following proposition.

Proposition 4.2. Consider the numerical scheme (4.1) with the positivity-preserving limiter (4.7) and θ computed in (4.8). Suppose the well-balanced flux (3.8) is used, with $\widetilde{H}_{j-\frac{1}{2}}^{*,+}, \widetilde{H}_{j+\frac{1}{2}}^{*, -}$ computed following (3.7). This method is high order accurate, positivity-preserving and conserves the mass, under the CFL condition (4.6). For a fifth-order WENO scheme with $k = 3$, this CFL condition is $\lambda\alpha \leq 1/12$.

We would like to mention that in wet regions, where Q_j is bigger than zero, the limiter does not take effect, i.e., $\widetilde{H}_{j+1/2}^\pm(x) = H_{j+1/2}^\pm(x)$. Therefore this positivity-preserving limiter is active only in the dry or nearly dry region. For high order time discretizations, we need to apply the limiter in each stage for a Runge–Kutta method or in each step for a multistep method. To be efficient, we could implement the time step restriction (4.6) only when a preliminary calculation to the next time step produces negative water height. We refer to [11,28] for other comments regarding this positivity-preserving limiter.

5. Numerical examples

In this section we present some numerical results of our positivity-preserving well-balanced WENO methods for the one-dimensional shallow water flows through channels. We will demonstrate the well-balanced property of the proposed

Table 5.1

L^1 and L^∞ errors for different precisions for the steady state solution in Section 5.1.

Precision	L^1 error		L^∞ error	
	H	Q	H	Q
Single	3.25E–08	1.63E–06	2.38E–07	1.05E–05
Double	7.24E–17	5.57E–15	4.44E–16	2.82E–14

WENO methods, and investigate their ability to capture the small perturbations of steady state solutions. We will also verify their positivity-preserving feature in handling wetting and drying test cases, and study the effect of variable cross section on the solutions. Fifth order finite volume WENO schemes, coupled with the fourth order source term approximation, are implemented as examples. We use the third order TVD Runge–Kutta time discretization (3.3) for the temporal discretization. Unless otherwise specified, the CFL number is taken as 0.08, to satisfy the positivity-preserving requirement $\lambda\alpha < 1/12$ in Proposition 4.2. In the practical application, to save computational time, one can use the regular WENO CFL number (for example, 0.8), and switch back to 0.08 only if the positivity of water cross section is violated. In the following examples, we fix the gravitation constant g as 9.812 m/s^2 . Unless otherwise stated, we consider the flows through the channels with varying width, which takes the form of

$$\sigma(x) = \begin{cases} 1 - \sigma_0 \left(1 + \cos \left(2\pi \frac{x - (x_l + x_r)/2}{x_r - x_l} \right) \right), & \text{if } x \in [x_l, x_r], \\ 1, & \text{otherwise.} \end{cases} \quad (5.1)$$

Here x_l and x_r are the left and right boundary of the contraction, and $1 - 2\sigma_0$ denotes the minimum width of the channel at the point $(x_l + x_r)/2$.

5.1. Test for the well-balanced property

The first test problem is chosen to verify the well-balanced property of our proposed WENO schemes, on a still water steady state problem with a non-flat bottom and non-constant cross section. The bottom topography is given by the depth function [14]

$$b(x) = \begin{cases} 0.25(1 + \cos(10\pi(x - 0.5))), & \text{if } 0.4 \leq x \leq 0.6, \\ 0, & \text{otherwise,} \end{cases}$$

in the domain $[0, 1]$, and the initial data is the still water steady state solution

$$h + b = 1, \quad Q = \sigma hu = 0.$$

The channel $\sigma(x)$ is given by (5.1) with $x_l = 0.25$, $x_r = 0.75$, and $\sigma_0 = 0.2$. With the periodic boundary condition, the steady state should be exactly preserved. We compute the solution until $t = 1$ using 200 uniform cells. The computed surface level $h + b$ (measured by $(H_j + \bar{B}_j)/\bar{\sigma}_j$) and the bottom b (measured by $\bar{B}_j/\bar{\sigma}_j$) are plotted in Fig. 5.1. In order to demonstrate that the still water steady state solution is maintained up to round-off error, we use single- and double-precision to perform the computation. The L^1 and L^∞ errors for the cross-sectional wet area H and the mass flow Q with different precisions are shown in Table 5.1. We can clearly see that the L^1 and L^∞ errors are both at the level of round-off errors for these precisions, which verify the desired well-balanced property. We have also tested with other choices of x_l , x_r and σ , and observe the same results.

5.2. Small perturbation tests

The following test case was first studied in [14], and is chosen here to demonstrate the capability of the proposed WENO scheme for computations on the small perturbation of a steady state solution, which cannot be captured well by a non-well-balanced scheme. We follow the setup in Section 5.1, and impose a small perturbation to the initial data:

$$h + b = \begin{cases} 1 + \epsilon, & \text{if } 0.1 \leq x \leq 0.2, \\ 1, & \text{otherwise,} \end{cases} \quad Q = \sigma hu = 0.$$

Theoretically, this small disturbance should split into two waves, propagating left and right at the characteristic speeds. Non-well-balanced numerical methods have difficulty with capturing such small perturbations of the water surface on a non-flat bottom topography, and we refer to [9, example 1] for some numerical results of non-well-balanced methods, where big oscillation can be observed. We have tested two different sets of channel $\sigma(x)$, one with a left shifted contraction $x_l = 0.15$, $x_r = 0.65$, $\sigma_0 = 0.2$, and the other with a right shifted contraction $x_l = 0.35$, $x_r = 0.85$, $\sigma_0 = 0.2$. The solutions at different times for the perturbation $\epsilon = 0.01$ on 200 uniform computational cells with simple transmissive boundary conditions, compared with 2000 cells “reference” solutions, are shown in Fig. 5.2. We can observe that the

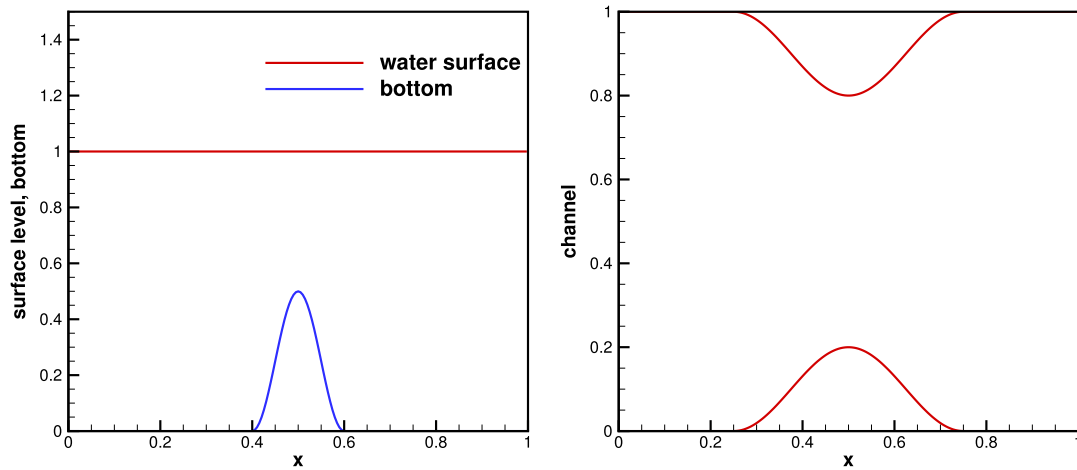


Fig. 5.1. The still water steady state solution in Section 5.1. Left: the surface level $h + b$ and the bottom topography b ; Right: the shape $\sigma(x)$ of the channel.

numerical solutions at the coarse mesh match the results on the refined mesh well, and there are no spurious numerical oscillations. With the difference shape of the channel, we can observe a slight different water surface level, especially the small perturbation wave propagating right at time $T = 0.05$ and 0.15 .

5.3. Oscillating lake test

The oscillating lake test was first proposed in [2] for the shallow water equations, and later modified in [14] for the shallow water flows through channels. This provides a good test case for inundating storm tides. Following the setup in [14], we set the domain as $[0, 1]$, and the channel $\sigma(x)$ is given by (5.1) with $x_l = 0.25$, $x_r = 0.75$, and $\sigma_0 = 0.1$. The non-flat bottom topography $b(x)$ takes the form of

$$b(x) = \frac{1}{4} (2 - (1 + \cos 2\pi(x - 0.5))),$$

and the initial condition contains a small sinusoidal perturbation from the still water steady state solution:

$$h(x) = \max(0, 0.4 + 0.04 \sin \kappa(x - 0.5) - b(x)), \quad u(x, 0) = 0,$$

with $\kappa = 4.0547$. Because the flow cannot reach the boundaries, we can pick any boundary conditions, which have no impact on the numerical solutions. The small perturbation oscillates, and produces a moving wetting and drying front on both shores of the lake. We run the simulation with 200 uniform cells, and present in Fig. 5.3 the solutions at time $T = 18.002$, which correspond to a time where the flow obtains its higher level on the left shore of the lake. The solutions compare well with that from [14]. This confirms the positivity-preserving property of our methods.

5.4. Drain on a non-flat bottom

This drainage numerical example aims to test the ability of the proposed method to deal with the dry areas over a non-flat bottom. It was first proposed by Gallouët et al. [30], and also appeared in [28]. The flow is computed in the domain of $[0, 25]$, and the left boundary condition is a free condition on H and zero on Q . The right boundary condition is an outlet condition on a dry bed (refer to [30] for the details). We consider the bottom topography

$$b(x) = \begin{cases} 0.2 - 0.05(x - 10)^2, & \text{if } 8 \leq x \leq 12, \\ 0, & \text{otherwise,} \end{cases}$$

with the channel parameters $x_l = 3.75$, $x_r = 16.25$, and $\sigma_0 = 0.2$. The initial data is a still flat water

$$h(x, 0) = 0.5 - b(x), \quad H(x, 0) = \sigma(x)h(x, 0), \quad hu(x, 0) = 0.$$

We use 250 uniform cells in the computation, and present the numerical solutions at different times $T = 10, 20, 100$ and 1000 in Figs. 5.4 and 5.5. Since the outlet boundary condition on the right allows the water to flow out of the domain on the right, a dry region is developed near the right side of the bump first. After a long time, the solution reaches a steady state, which is a still water on the left of the bump, and a dry state on the right. This is a challenging numerical example, as it requires the numerical methods to be both well-balanced and positivity-preserving to capture the expected steady state well. Our numerical solutions reflect this pattern well and converge to the steady state.

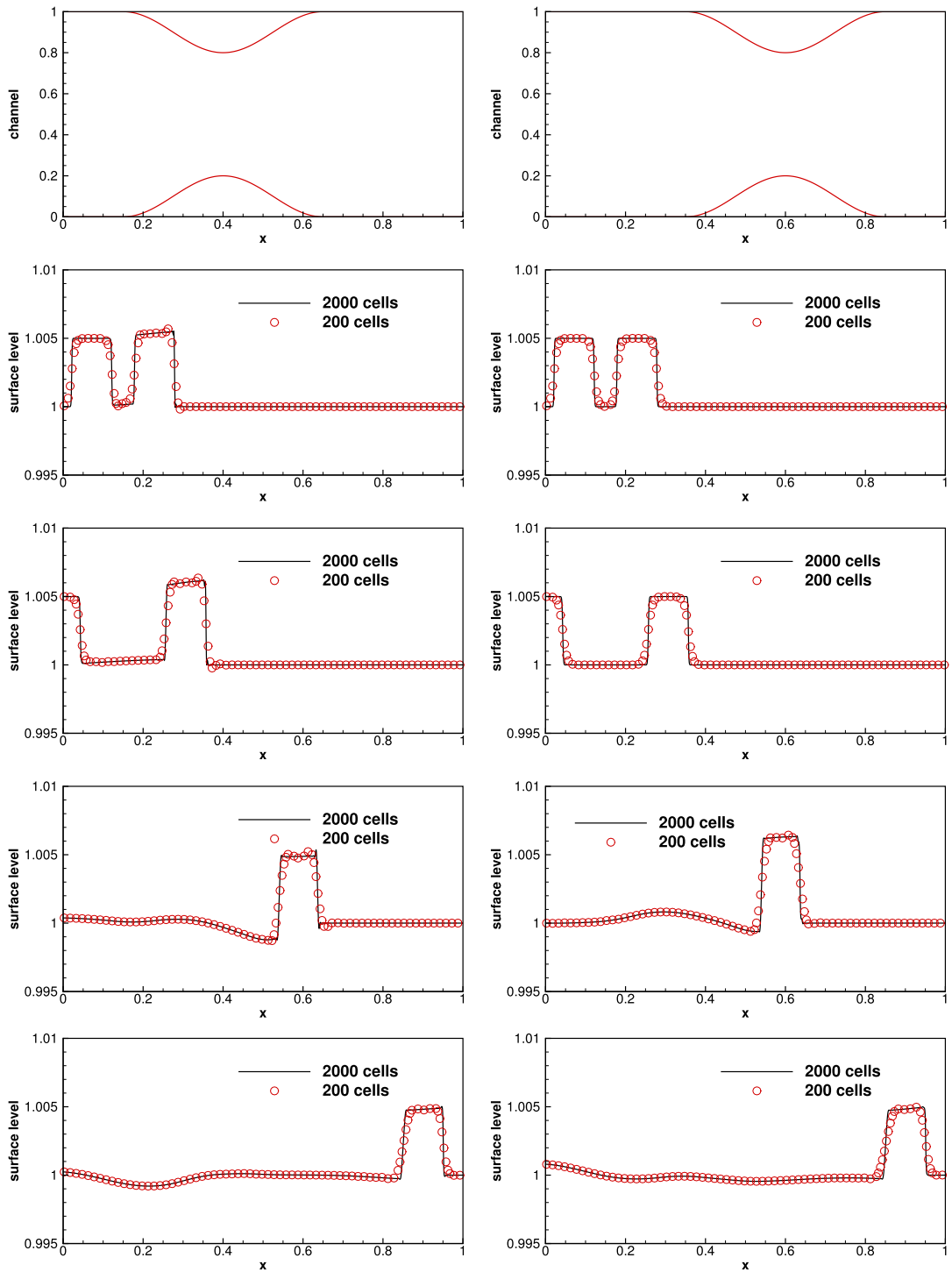


Fig. 5.2. The contracting channel $\sigma(x)$ (the top row) and the water surface level $h + b$ in the small perturbation test ($\epsilon = 0.01$) of a steady state solution at various times $T = 0.025, 0.05, 0.15$ and 0.25 (from top to bottom) in Section 5.2. Left: the channel with a left shifted contraction; Right: the channel with a right shifted contraction.

5.5. A converging–diverging channel

In this example, we consider the classic transcritical steady flow test on a flat bottom in a converging–diverging channel, originally proposed by García-Navarro et al. in [31]. This is related to many practical problems such as flow between bridge piers.

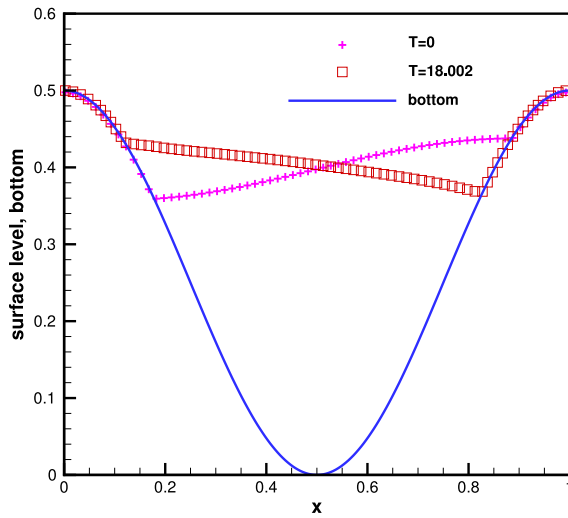


Fig. 5.3. Oscillating lake test in Section 5.3. Initial water surface, water surface at $T=18.002$, and bottom topography.

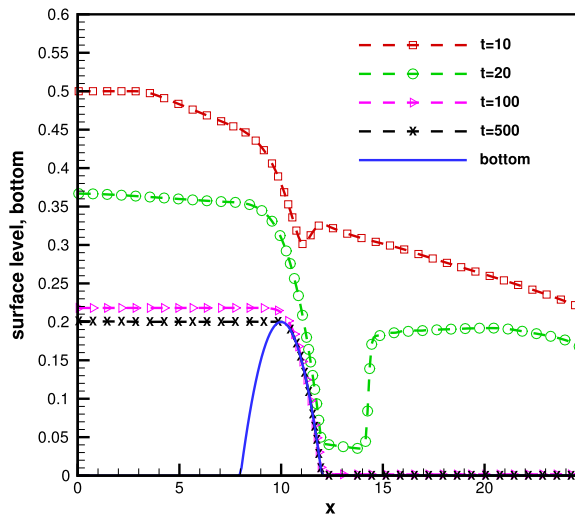


Fig. 5.4. Drain on a non-flat bottom in Section 5.4. The surface level at different time.

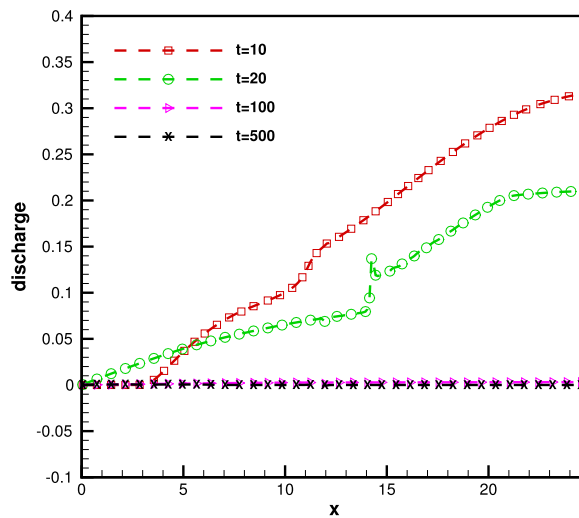


Fig. 5.5. Drain on a non-flat bottom in Section 5.4. The discharge at different time.

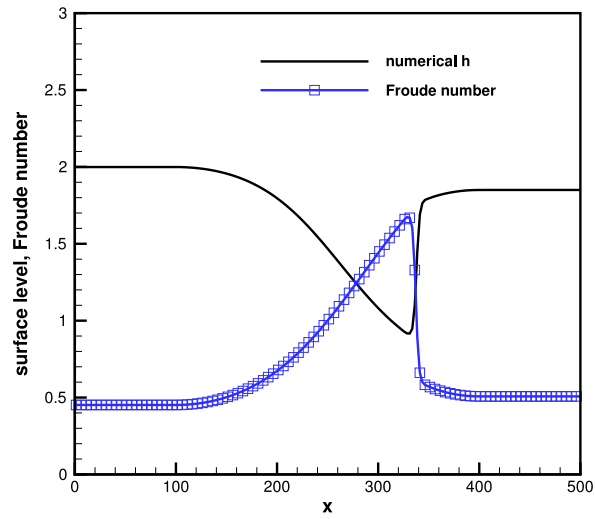


Fig. 5.6. Steady transcritical flow in a converging–diverging channel in Section 5.5.

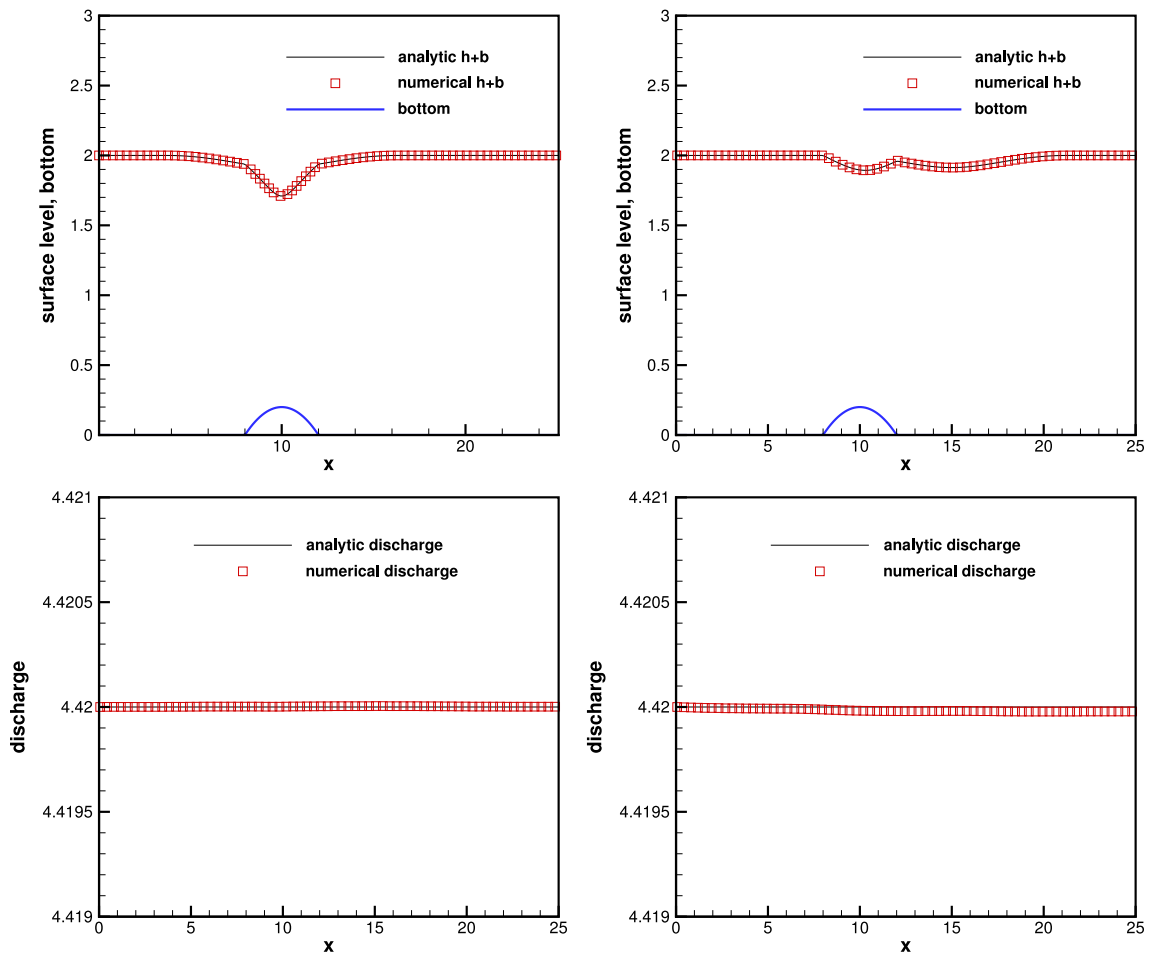


Fig. 5.7. Steady subcritical flow over a bump in Section 5.6. Top: the surface level $h + b$; bottom: the discharge Q as the numerical flux for the water height H ; Left: the channel with a left shifted contraction; Right: the channel with a right shifted contraction.

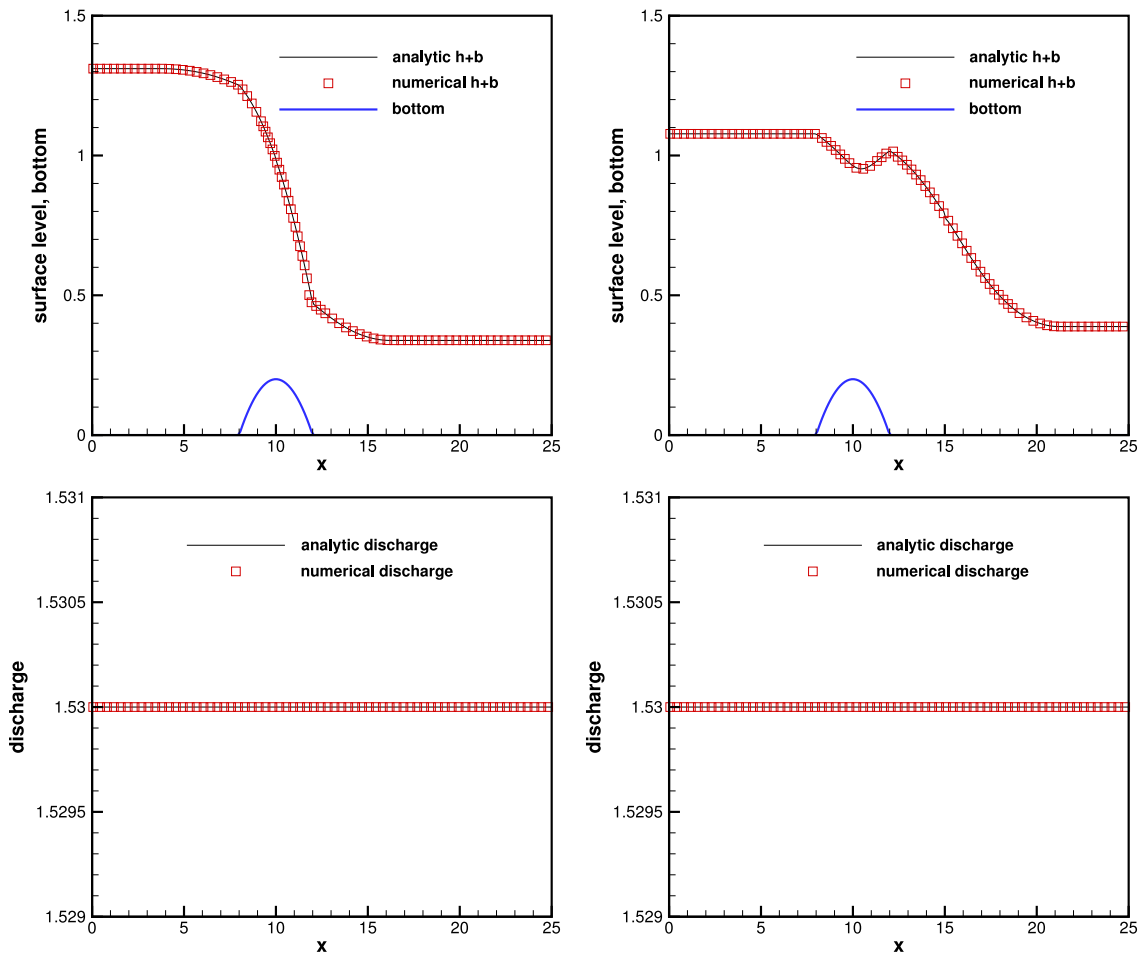


Fig. 5.8. Steady transcritical flow over a bump without a shock in Section 5.6. Top: the surface level $h + b$; bottom: the discharge Q as the numerical flux for the water height H ; Left: the channel with a left shifted contraction; Right: the channel with a right shifted contraction.

The computational domain is defined on the converging–diverging channel of length 500, with the width variation of the channel defined by

$$\sigma(x) = \begin{cases} 5 - 0.7065 \left(1 + \cos \left(2\pi \frac{x - 250}{300} \right) \right), & \text{if } x \in [150, 450], \\ 5, & \text{otherwise.} \end{cases}$$

The bottom topography is assumed to flat (i.e., $b = 0$), and the initial conditions are given by

$$h = 2, \quad Q = \sigma hu = 20.$$

together with the boundary condition of $Q = 20$ at the upstream, and $h = 1.85$ at the downstream. We run the simulation with 200 uniform cells for a long time until it reaches the steady state. The numerical results at time $T = 5000$ are shown in Fig. 5.6, where we can observe the water surface decreases first. At the point of maximum contraction ($x = 250$), the flow reaches the critical point where it changes from subcritical to supercritical flow. A stationary hydraulic jump appears later to connect to the subcritical downstream boundary condition. The numerical results match well with those in [31,12].

5.6. Moving steady states over a hump

The purpose of this test case is to study the convergence in time of the proposed methods towards steady flow over a non-flat bump with various channel configurations. These are classical test problems for transcritical and subcritical flows, and are widely used to test numerical schemes for shallow water equations.

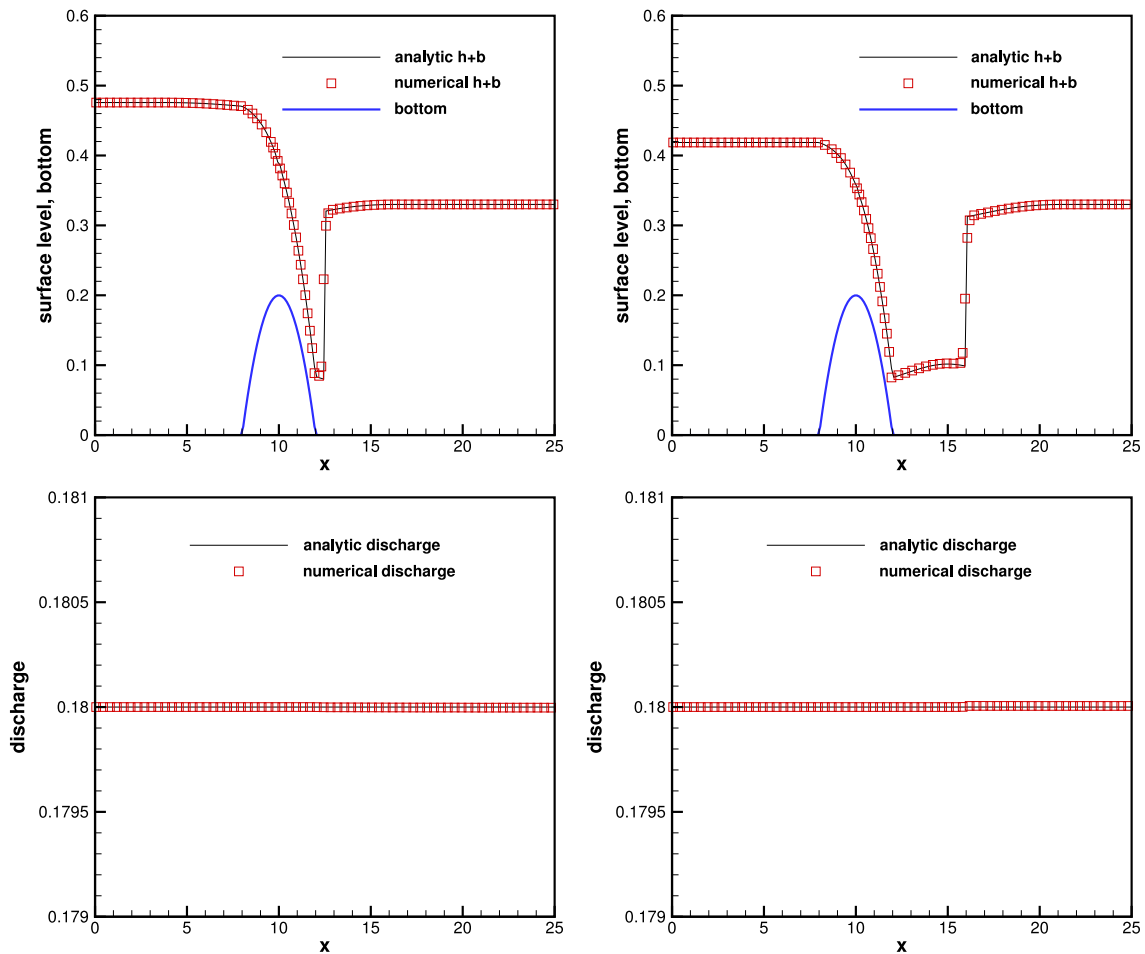


Fig. 5.9. Steady transcritical flow over a bump with a shock in Section 5.6. Top: the surface level $h + b$; bottom: the discharge Q as the numerical flux for the water height H ; Left: the channel with a left shifted contraction; Right: the channel with a right shifted contraction.

Here we follow the setup presented in [22], where the same tests are studied for the constant width channel case. The bottom function is given by:

$$b(x) = \begin{cases} 0.2 - 0.05(x - 10)^2, & \text{if } 8 \leq x \leq 12, \\ 0, & \text{otherwise,} \end{cases}$$

for a channel of length 25, and the initial conditions are taken as

$$h(x, 0) = 0.5 - b(x) \quad \text{and} \quad Q(x, 0) = 0.$$

Depending on different boundary conditions, the flow can be subcritical or transcritical with or without a steady shock. For all three cases, we use 200 uniform computational cells and set the final time as $t = 200$. Two sets of variable channel width will be tested to demonstrate the effect of channel on the final solutions. Analytical solutions for these moving water steady states can be computed, and will be shown in the figures to provide a comparison.

(a) Subcritical flow.

We set the boundary condition to $hu = 4.42$ at the upstream, and $h = 2$ at the downstream, and this will evolve to a moving water steady state which is a subcritical flow. We have tested two different sets of channel $\sigma(x)$, one with a left shifted contraction $x_l = 3.75, x_r = 16.25, \sigma_0 = 0.05$, and the other with a right shifted contraction $x_l = 8.75, x_r = 21.25, \sigma_0 = 0.05$. If the channel contraction is not too narrow, the flow remains subcritical. The surface level $h + b$ and the discharge Q , are plotted in Fig. 5.7, which are in good agreement with the analytical solution. The correct capturing of the discharge Q is usually more difficult than the surface level $h + b$, as noticed by many authors. We can also observe the effect of different channel shapes on the final solutions.

(b) Transcritical flow without a shock.

We set the boundary condition to $hu = 1.53$ at the upstream, and $h = 0.66$ at the downstream when the flow is subsonic. We have tested two different sets of channel $\sigma(x)$, one with a left shifted contraction $x_l = 3.75, x_r =$

- 16.25, $\sigma_0 = 0.15$, and the other with a right shifted contraction $x_l = 8.75$, $x_r = 21.25$, $\sigma_0 = 0.15$. The surface level $h + b$ and the discharge Q are plotted in Fig. 5.8, which show very good agreement with the analytical solution.
- (c) Transcritical flow with a shock.

We set the boundary condition to $hu = 0.18$ at the upstream, and $h = 0.33$ at the downstream. We have tested two different sets of channel $\sigma(x)$, one with a left shifted contraction $x_l = 3.75$, $x_r = 16.25$, $\sigma_0 = 0.15$, and the other with a right shifted contraction $x_l = 8.75$, $x_r = 21.25$, $\sigma_0 = 0.15$. In the long time steady state solution, a shock appears in the middle of the domain. The surface level $h + b$ and the discharge Q are plotted in Fig. 5.9, which show very good agreement with the analytical solution.

6. Concluding remarks

In this paper, we have constructed well-balanced and positivity-preserving finite volume WENO methods for the shallow water flows in open channels with irregular geometry. Well-balanced properties are obtained by a novel high order source term approximation using the extrapolation technique, as well as the well-balanced numerical fluxes. A simple positivity-preserving limiter is introduced to ensure the resulting methods maintain the non-negativity of the cross-sectional wet area. This positivity-preserving limiter can preserve the mass conservation, is easy to implement, and at the same time does not affect the high order accuracy for the general solutions. Extensive numerical examples are provided to demonstrate the performance of the proposed methods. Extension to shallow water flows in channel with general cross section constitutes our future work.

Acknowledgment

Research is partially sponsored by National Science Foundation grant DMS-1216454.

References

- [1] A. Bermudez, M.E. Vazquez, Upwind methods for hyperbolic conservation laws with source terms, *Comput. & Fluids* 23 (1994) 1049–1071.
- [2] E. Audusse, F. Bouchut, M.-O. Bristeau, R. Klein, B. Perthame, A fast and stable well-balanced scheme with hydrostatic reconstruction for shallow water flows, *SIAM J. Sci. Comput.* 25 (2004) 2050–2065.
- [3] R.J. LeVeque, Balancing source terms and flux gradients on high-resolution Godunov methods: the quasi-steady wave-propagation algorithm, *J. Comput. Phys.* 146 (1998) 346–365.
- [4] B. Perthame, C. Simeoni, A kinetic scheme for the Saint-Venant system with a source term, *Calcolo* 38 (2001) 201–231.
- [5] Y. Xing, C.-W. Shu, High order finite difference WENO schemes with the exact conservation property for the shallow water equations, *J. Comput. Phys.* 208 (2005) 206–227.
- [6] Y. Xing, Exactly well-balanced discontinuous galerkin methods for the shallow water equations with moving water equilibrium, *J. Comput. Phys.* 257 (2014) 536–553.
- [7] O. Bokhove, Flooding and drying in discontinuous Galerkin finite-element discretizations of shallow-water equations. Part 1: one dimension, *J. Sci. Comput.* 22 (2005) 47–82.
- [8] A. Ern, S. Piperno, K. Djadel, A well-balanced Runge–Kutta discontinuous Galerkin method for the shallow-water equations with flooding and drying, *Internat. J. Numer. Methods Fluids* 58 (2008) 1–25.
- [9] A. Kurganov, D. Levy, Central-upwind schemes for the Saint-Venant system, *M2AN Math. Model. Numer. Anal.* 36 (2002) 397–425.
- [10] S. Bunya, E.J. Kubatko, J.J. Westerink, C. Dawson, A wetting and drying treatment for the Runge–Kutta discontinuous Galerkin solution to the shallow water equations, *Comput. Methods Appl. Mech. Engrg.* 198 (2009) 1548–1562.
- [11] Y. Xing, X. Zhang, C.-W. Shu, Positivity-preserving high order well-balanced discontinuous Galerkin methods for the shallow water equations, *Adv. Water Resour.* 33 (2010) 1476–1493.
- [12] M.E. Vazquez-Cendon, Improved treatment of source terms in upwind schemes for the shallow water equations in channels with irregular geometry, *J. Comput. Phys.* 148 (1999) 497–526.
- [13] P. Garcia-Navarro, M.E. Vazquez-Cendon, On numerical treatment of the source terms in the shallow water equations, *Comput. & Fluids* 29 (2000) 951–979.
- [14] J. Balbas, S. Karni, A central scheme for shallow water flows along channels with irregular geometry, *ESAIM Math. Model. Numer. Anal.* 43 (2009) 333–351.
- [15] G. Hernández-Duenas, S. Karni, Shallow water flows in channels, *J. Sci. Comput.* 48 (2011) 190–208.
- [16] J. Murillo, P. Garcia-Navarro, Accurate numerical modeling of 1D flow in channels with arbitrary shape. application of the energy balanced property, *J. Comput. Phys.* 260 (2014) 222–248.
- [17] M.J. Castro, J.M. Gallardo, C. Parés, High order finite volume schemes based on reconstruction of states for solving hyperbolic systems with nonconservative products. applications to shallow-water systems, *Math. Comp.* 75 (2006) 1103–1134.
- [18] R. Abgrall, S. Karni, A comment on the computation of non-conservative products, *J. Comput. Phys.* 229 (2010) 2759–2763.
- [19] G. Jiang, C.-W. Shu, Efficient implementation of weighted ENO schemes, *J. Comput. Phys.* 126 (1996) 202–228.
- [20] C.-W. Shu, Essentially non-oscillatory and weighted essentially non-oscillatory schemes for hyperbolic conservation laws, in: A. Quarteroni (Ed.), *Advanced Numerical Approximation of Nonlinear Hyperbolic Equations*, in: *Lecture Notes in Mathematics*, vol. 1697, Springer, 1998, pp. 325–432.
- [21] C.-W. Shu, S. Osher, Efficient implementation of essentially non-oscillatory shock-capturing schemes, *J. Comput. Phys.* 77 (1988) 439–471.
- [22] Y. Xing, C.-W. Shu, High order well-balanced finite volume WENO schemes and discontinuous Galerkin methods for a class of hyperbolic systems with source terms, *J. Comput. Phys.* 214 (2006) 567–598.
- [23] Y. Xing, C.-W. Shu, A new approach of high order well-balanced finite volume WENO schemes and discontinuous Galerkin methods for a class of hyperbolic systems with source terms, *Commun. Comput. Phys.* 1 (2006) 100–134.
- [24] S. Noelle, N. Pankratz, G. Puppo, J.R. Natvig, Well-balanced finite volume schemes of arbitrary order of accuracy for shallow water flows, *J. Comput. Phys.* 213 (2006) 474–499.
- [25] S. Noelle, Y. Xing, C.-W. Shu, High-order well-balanced finite volume WENO schemes for shallow water equation with moving water, *J. Comput. Phys.* 226 (2007) 29–58.
- [26] X. Zhang, C.-W. Shu, On maximum-principle-satisfying high order schemes for scalar conservation laws, *J. Comput. Phys.* 229 (2010) 3091–3120.
- [27] Y. Xing, X. Zhang, Positivity-preserving well-balanced discontinuous Galerkin methods for the shallow water equations on unstructured triangular meshes, *J. Sci. Comput.* 57 (2013) 19–41.

- [28] Y. Xing, C.-W. Shu, High-order finite volume WENO schemes for the shallow water equations with dry states, *Adv. Water Resour.* 34 (2011) 1026–1038.
- [29] C.-W. Shu, Total-variation-diminishing time discretizations, *SIAM J. Sci. Stat. Comput.* 9 (1988) 1073–1084.
- [30] T. Gallouët, J.-M. Hérard, N. Seguin, Some approximate Godunov schemes to compute shallow-water equations with topography, *Comput. & Fluids* 32 (2003) 479–513.
- [31] P. GarcíaNavarro, F. Alcrudo, J. Savirón, 1D open channel flow simulation using TVD-McCormack scheme, *J. Hydraul. Eng.* 118 (1992) 1359–1372.